

Photocatalytic treatment of oil and grease spills in wastewater using coated N-doped TiO₂ polyscales under sunlight as an alternative driving energy

H. P. Shivaraju¹ · N. Muzakkira¹ · B. Shahmoradi²

Received: 5 February 2016/Revised: 4 May 2016/Accepted: 30 May 2016/Published online: 9 June 2016
© Islamic Azad University (IAU) 2016

Abstract To enhance the overall efficiency of oil and grease removal in wastewater coated N-doped TiO₂ photocatalytic polyscales were fabricated through sol–gel technique. The materials fabricated were characterized using powder X-ray diffraction, Fourier transmission infrared spectroscopy, scanning electron microscopy, and UV–Vis spectroscopy. In order to enhance degradation efficiency of organic pollutant under natural sun light, shifting of absorption range of TiO₂ to visible spectrum, various modifications such as surface modification and size optimization were carried out by doping of nitrogen under sol–gel processes. To ease recovery of suspended catalysts from aqueous media, the coated N-doped TiO₂ were prepared by decorating photocatalytic particles onto suitable substrates. N-doped TiO₂ polyscales with desired functionalities were coated onto the spherical supporting substrates using a binding agent. The photocatalytic treatment studies clearly indicated the considerable level of the oil and grease and other organic pollutants removal from wastewater (up to 85–90 % ± 2) using coated N-doped TiO₂ under natural sunlight as an alternative driving energy source. Removal of oil and grease along with other organic pollutants in wastewater using coated N-doped TiO₂ polyscales is a versatile, economical, and environmental friendly technique due to the ease of handling and recovery, utilization of natural sunlight which is renewable energy source.

Keywords Photocatalyst · Wastewater · Sol–gel · TiO₂ · Oil and grease · Coating · Natural sunlight

Introduction

Nowadays water treatment is expensive, and new technology is needed for the sustainable reclamation and reuse of polluted water and wastewater (Zekker et al. 2012, 2013, 2014, 2015a, b; Rodrigo et al. 2016; Ergo et al. 2014; Sadler et al. 1994). Due to drastic modernization and urbanizations, the use of petroleum oil and grease products for its energy need at industrial and anthropogenic activities has been increased drastically which led oil and grease pollution in water bodies (Hassan 1989; Rosario et al. 2003; Agota et al. 2012; Olumide et al. 2011; Zekker et al. 2012, 2014). Oil and grease is pollution caused by many sources such as accidental oil spills, leaks, industrial discharges, automobile discharge, and sewage, during chronic and careless usage of oil and oil products (Hassan 1989; Rosario et al. 2003). Some of the accidental incidents with tankers and leakage clearly demonstrated that oil contamination in an environmentally or economically sensitive area which could cause irreparable damage (Hassan 1989; Rosario et al. 2003; Agota et al. 2012; Olumide et al. 2011). It is estimated that 1.7 to 8.8 million metric tons of oil and grease contaminants are released into the world's water bodies every year (National academy of sciences 1985; Cooney 1984), of which >90 % is directly related to human activities (O'Brien and Peter 1976). It is also estimated that about 30 % of the oil and grease enters freshwater systems (Cooney 1984; Gennaro 2004; Brubaker 1993; Stolzenbach et al. 1977) and they could also affect the water quality by forming a layer of floating film, which causes a decrease in the gas exchange of the air and water

✉ H. P. Shivaraju
shivarajuenvi@gmail.com

¹ Department of Water and Health, Faculty of Life Sciences, JSS University, Mysore 570015, India

² Environmental Health Research Center, Kurdistan University of Medical Sciences, Sanandaj, Iran

body (Lepo et al. 2003; Adeola et al. 2012; Willard et al. 1995; Savita and Suchi 2007). Oil and grease pollution in fresh water bodies are very common, with >5000 oil spills taking place each year in the inland water of continental India (Savita and Suchi 2007; Laszlo et al. 2015). Such pollution can also affect aquatic life as well as human activities in the area of fisheries by damaging fishing boats, fishing gear, and floating fishing equipment (Savita and Suchi 2007). Unfortunately, conventional water treatment techniques are unable to remove oil and grease contamination completely and those techniques have some drawbacks such as time-consuming, costly, and long processes (Laszlo et al. 2015; Syed 2015; Kulik et al. 2007; Suresh Kumar et al. 1996; Zekker et al. 2016). Photocatalytic oxidation is the process in which oil and grease oxidize into carbon dioxide, water, and salts by a catalyst using light as driving energies without producing any residues. Catalyst-assisted advanced oxidation processes (AOPs) form hydroxyl radicals in aqueous media, and hydroxyl radicals are highly reactive with high oxidation potential ($E^0 = 2.8$ V) and nonselective substances to degrade petroleum hydrocarbon compounds (Pera-Titus et al. 2004; Andreozzi et al. 1999), and this is able to react with all types of oil contaminants. Titanium dioxide (TiO_2) is widely used photocatalyst in AOPs due to its chemical stability, wide availability, and potential interest as photocatalyst with bandgap energy of ~ 3.3 eV. Visible light responsive TiO_2 by doped metals or nonmetal ions into TiO_2 system can explain bandgap energy tunings for the visible ranges that emphasize the utilization of natural sunlight as an alternative driving energy. There are various advantages in modification of TiO_2 by doping with nitrogen such as narrowing of bandgap tuning toward absorbing visible light, enhanced impurity energy levels, and mitigating the recombination processes (Asahi et al. 2001; Irie et al. 2003; Ihara et al. 2003; Mehmet et al. 2014a, b; Vinod et al. 2015). Also, immobilization of photocatalytic particles on the surface of suitable supporting materials is the best choice for instance when compared to slurry form, because a much faster reaction rate is achieved by individual particles without aggregation. In addition, easy recovery of the photocatalysts reduces the operation cost of treatment and increases the degradation efficiency of contaminants by easy illumination to the light sources (Shivaraju et al. 2010a, b, Shivaraju 2011).

Hence, the aim of this study was to enhance photocatalytic degradation of oily wastewater using N-doped TiO_2 polyscales under natural sunlight illumination as an alternative driving energy. In addition, effective recovery of suspended photocatalytic particles from aqueous media using suitable supporting materials which reduces the operation cost and enhances the illumination efficiency.

Supported N-doped TiO_2 polyscales could be attributed in the continuous utilization and ease recovery of photocatalyst after treatment of oily wastewater which emphasizes the sustainable route of wastewater treatment.

Materials and methods

Preparation of photocatalytic materials

N-doped TiO_2 polyscale was prepared through sol-gel method using 10 ml of titanium tetra isopropoxide (TTIP) and a mixture of deionized water (25 ml) and alcohol (25 ml) under continuous mixing on a magnetic stirrer at ambient temperature. A small amount of ammonia was added into the mixture as a dopant (N) source, and then, it was kept for completion of the reaction along with continuous stirring (1500 rpm) for 5 h. The product was kept for aging for 24 h without any disturbance. Finally, the mixture was dried at 50°C for 24 h in a dust-free hot air oven. Impurities were removed from the obtained product by continuous washing with double-distilled water and then dried at room temperature. The resultant product was calcinated in a muffle furnace at 450°C for 2 h using a silica vessel with airtight lid. Coating N-doped TiO_2 particles onto the substrate was accomplished using fevicol as an effective binding agent. Later, the fabrication was continued by rapid mixing 2–3 drops of binder with 5 g of porous spherical ceramic beads (1–2 mm in size) and suddenly decorated by daubing approximately 1 g of N-doped TiO_2 polyscale. The prepared N-doped TiO_2 polyscale was dried under dust-free environment at room temperature. The same procedure was followed for the preparation of coated N-doped TiO_2 polyscale using thermocol beads (3–4 mm in size) as the supporting substrates.

Characterization of coated N-doped TiO_2 polyscales

The prepared N-doped TiO_2 polyscales were characterized using different analytical techniques to study the obtained features such as absorption band shift, crystallinity, structural elucidation, surface morphology, and photocatalytic activities. The analytical techniques like UV-Visible spectroscopy (Shimadzu UV-2100), Powder X-ray diffraction (XRD) (Rigaku Smart lab), Fourier transform infrared spectroscopy (FTIR) (Shimadzu-8400S), and Scanning electron microscopy (SEM) (JEOL USA JSM-6390LV) were used to characterize coated N-doped TiO_2 polyscales. Stability of decorated photocatalytic particles onto the substrate in an aqueous medium was studied by weight loss experiments under different speeds.

Photocatalytic degradation study

The photocatalytic activity of coated N-doped TiO₂ polyscales was determined using brilliant green dye-C₂₇-H₃₄N₂O₄S (Himedia, laboratory grade) in the aqueous medium. About 50 ml of diluted dye solution was taken in a 100-ml reaction vessel, and a known amount of coated N-doped TiO₂ polyscales was added into the dye solution under continuous stirring (150 rpm/m) using magnetic stirrer. The whole setup of the reaction vessel was kept under the visible light source (100 W tungsten bulbs) as an energy source for 6-h irradiation time. Initial and final concentration of dye solution was measured by spectrometric technique at $\lambda_{\max} = 420$ nm and standard calibration curve. The schematic of photocatalytic degradation experimental setup is shown in Fig. 1. The experimental setup constituted with 100 ml quartz vessel provided with lid and content of the vessel was stirred by means of a magnetic stirrer (Remi, India). Decreased concentration of dye solution (C) confirms the breakdown of dye molecules under the photocatalytic activities of coated N-doped TiO₂ polyscales. The photocatalytic degradation efficiency was calculated using Eq. 1.

$$\text{Photocatalytic degradation rate (\%)} = \frac{C_i - C_f}{C_i} \times 100 \quad (1)$$

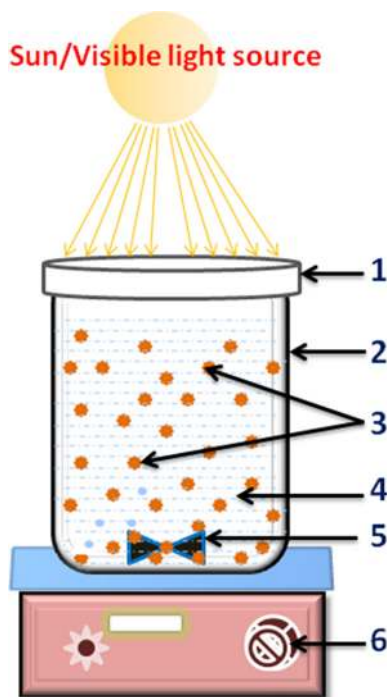


Fig. 1 Schematic of photocatalytic degradation experimental setup under visible light illumination: Silica lid-1; Reaction vessel-2; N-doped TiO₂ coated beads-3; Wastewater-4; Teflon-coated stirrer bar-5; Stirrer speed controller-6

where C_i is the dye initial concentration and C_f is the dye final concentration. Estimation of the photocatalytic degradation of oil and grease using coated N-doped TiO₂ polyscales was carried out under natural sunlight illumination. During the photocatalytic experiments under natural sunlight, exposure value of sunlight luminance was recorded frequently using lux light meter (Equinox EQ-1301). During the degradation study, approximately 1 g of coated N-doped TiO₂ polyscales was added into a 200 ml of model aqueous solution containing only 25 mg/l oil and grease in the reaction vessel. The irradiation time was varied from 6 to 24 h, and a blank experiment was also carried out without adding coated N-doped TiO₂ polyscales. Quantitative estimation of initial and final concentration of oil and grease in aqueous media was carried out by partition gravimetric method (APHA, AWWA, and WEF 2015). Photocatalytic degradation rate (%) was calculated using Eq. 2.

$$\text{Photocatalytic degradation rate of oil and grease (\%)} = \frac{OG_i - OG_f}{OG_i} \times 100 \quad (2)$$

where OG_i is initial weight of oil and grease and OG_f is the final weight of oil and grease.

Photocatalytic degradation of oil and grease in the real-time wastewater was determined using coated N-doped TiO₂ polyscales. The real-time wastewater sample was collected from the outlet of large-scale automobile service stations in Mysore City, India. The experiments were carried out by following above-mentioned procedure for 24-h irradiation time under natural sunlight. In addition to oil and grease removal potential, the chemical oxygen demand (COD) removal efficiency was also considered as an important parameter to determine the degradation efficiency of N-doped TiO₂ polyscales in the real-time wastewater. Determination of initial (10,400 mg/l) and final COD in the wastewater was carried out by standard analytical method (APHA, AWWA, and WEF 2015), and COD was analyzed 1-h intervals. The removal rate of COD by coated N-doped TiO₂ polyscales was calculated using Eq. 3.

$$\text{Photocatalytic removal rate of COD (\%)} = \frac{COD_i - COD_f}{COD_i} \times 100 \quad (3)$$

where COD_i and COD_f are initial and final CODs, respectively.

Results and discussion

The coated polyscales were prepared using N-doped TiO₂ particles; thermocol and ceramic beads were used as potential supporting substrates, which are less dense,

spherical in shape, and porous in nature. Among thermocol and ceramic beads, ceramic beads ($<0.89 \text{ g/cm}^3$ density) were comparatively highly porous in nature than thermocol beads ($<0.67 \text{ g/cm}^3$ density) and vice versa in case of density. Photocatalytic degradation efficiency of coated N-doped TiO_2 polyscales was tested by the treatment of oil and grease in aqueous medium under natural sunlight illumination as a driving energy source.

Characteristics of coated N-doped TiO_2 polyscales

Coated N-doped TiO_2 polyscales were synthesized through sol–gel technique, and as-prepared polyscales were characterized using suitable analytical techniques. The optical and band shifting characteristics of coated N-doped TiO_2 polyscales were investigated using UV–Visible spectrophotometer, and the results were compared with pure TiO_2 particles. The UV–Visible absorption spectrum of coated N-doped TiO_2 polyscales and pure TiO_2 particles are depicted in Fig. 2. The spectrum of coated N-doped TiO_2 polyscales and TiO_2 particles exhibited a strong absorption band between 360–400 and 387 nm that is near UV region, respectively. Coated N-doped TiO_2 polyscale showed two absorption edges at 386 and 397.8 nm that are in the range of visible spectra. The optical absorption edges of coated N-doped TiO_2 polyscales showed considerably shifted edges near the visible region when compared to pure TiO_2 . The shift in the absorption edge to smaller photon energy implies a decreased energy level in the conduction band, and a consequent narrowing of the bandgap (Asahi et al. 2001; Irie et al. 2003; Ihara et al. 2003). This shifting in their absorption edge near the visible region clearly implies

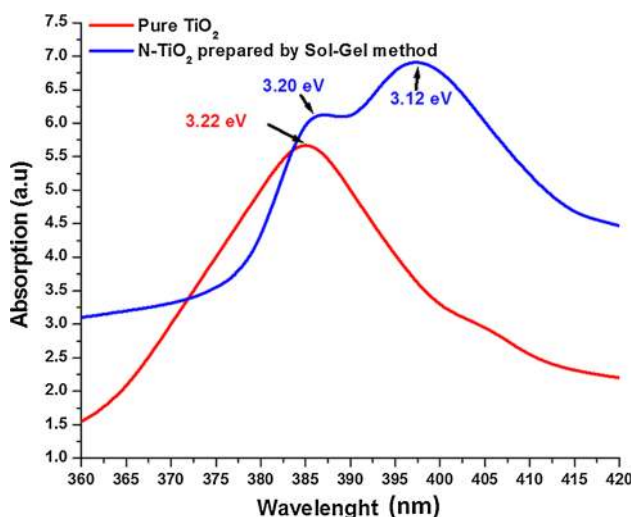


Fig. 2 UV–Visible spectra of N-doped TiO_2 polyscales and pure TiO_2 particles

band tuning coated N-doped TiO_2 polyscales using sol–gel technique. Coated N-doped TiO_2 polyscales showed a consequent narrowing of the bandgap from 3.22 eV to 3.20 and 3.12 eV; it induces the apparent activation of coated N-doped TiO_2 polyscales under natural sunlight illumination that consists with 90 and 10 % of visible and UV light, respectively. Powder X-ray diffraction pattern was recorded over a 2θ range of 10–80 with a speed of 3° per minutes using a nickel-filtered $\text{Cu K}\alpha$ radiation source. In Fig. 3, spectra (a) and (b) indicated the powder X-ray diffraction pattern of pure TiO_2 and coated N-doped TiO_2 polyscales, respectively, which are dominantly indexed to JCPDS files 84–1285 (Emerson et al. 2015; Gomathi Devi and Kavitha 2014; Shivaraju et al. 2010a, b). The XRD pattern of coated N-doped TiO_2 polyscales confirmed the anatase phase and characteristic peak of anatase is sharp and clearly observed particularly at 2θ of 25.2. The XRD pattern of coated N-doped TiO_2 polyscales indicated increased peak intensity that induces well-crystalline phase when compared to pure TiO_2 . Well-crystalline phase of coated N-doped TiO_2 polyscales is apparently stable and enhances the photocatalytic activities (Gomathi Devi and Kavitha 2014).

Figure 4 shows the FTIR spectrum of coated N-doped TiO_2 polyscales, and it indicates the stretching vibration of O–H bond from hydroxyl at 3417.24 cm^{-1} . FTIR peak at 1639.3 cm^{-1} indicates the O–H bending of molecularly physisorbed water, and the C=O stretching mode of vibration is observed at 1570 cm^{-1} . For a linear molecule such as absorbed CO or CO_2 , stretching mode of vibration is observed at 2340 to 2380 cm^{-1} and the molecule remains linear throughout the vibration. Nonlinear molecules usually have three different moments of inertia. In this case, the vibration rotation spectrum can be very

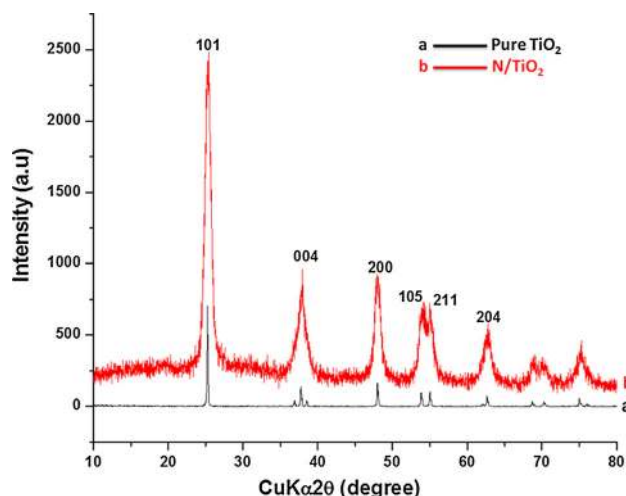
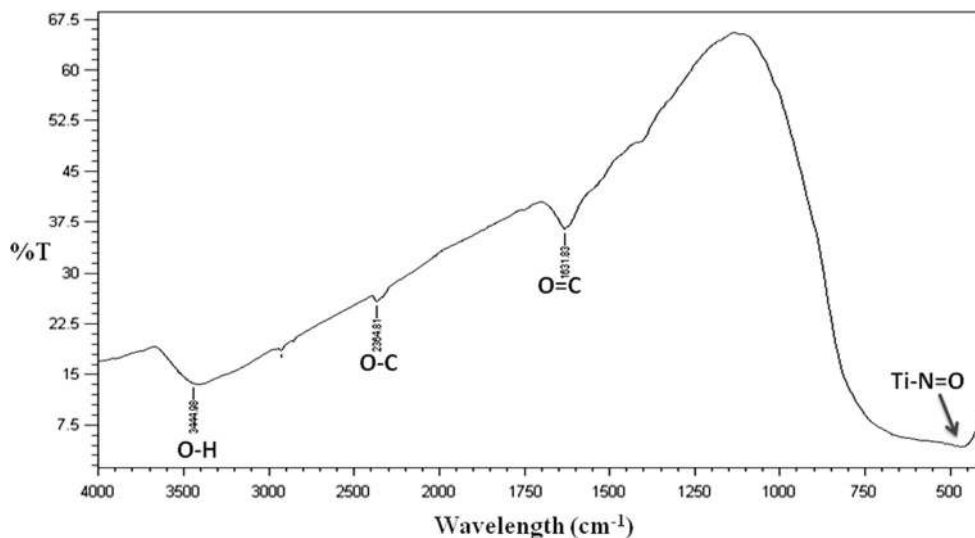
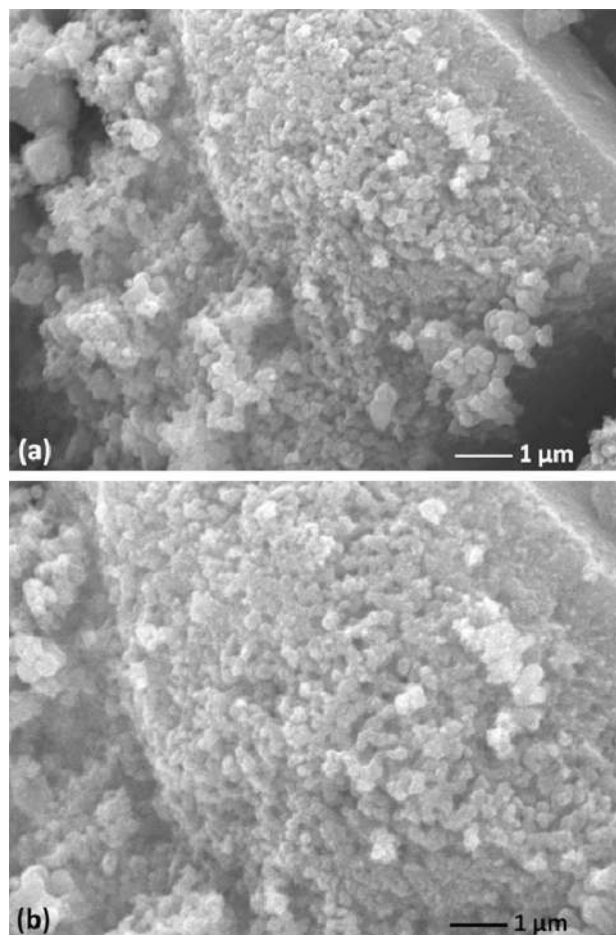


Fig. 3 Powder X-ray diffraction patterns of **a** TiO_2 , **b** coated N-doped TiO_2 polyscales

Fig. 4 FTIR spectrum of coated N-doped TiO₂ polyscales

complex, even for a simple molecule such as water. The rotational fine structure of the H–O–H bending mode of water is commonly observed at the range in 1200 to 2000 cm^{-1} (1500 cm^{-1}). Since water is a most polar solvent, bands of solutes in aqueous solution are usually broader than in any other solvent. When functional groups such as O–H are hydrogen-bonded, the width of the stretching bands may be $>100 \text{ cm}^{-1}$. The bands in near-infrared spectra are overtones or combinations of fundamentals (C–H, O–H and N–H); the widths of these bands are typically greater than the widths of bands from which they are derived (Gomathi Devi and Kavitha 2014; Shivaraju et al. 2010a, b). A characteristic band with strong and wide absorption at lower energy region ($<420 \text{ cm}^{-1}$) is attributed to the formation of anatase O–Ti–O lattice. The stretching band corresponding to the nitrogen in the lattice structure (Ti–N=O) may be identified at lower energy absorption region in the spectrum.

The SEM image was used to determine the morphology of coated N-doped TiO₂ polyscales. The growth of mixed and agglomerated spherical shaped particles of coated N-doped TiO₂ polyscales can be clearly seen in Fig. 5. This SEM indicates that coated N-doped TiO₂ polyscales have spherical morphology creating high surface area and porosity, which is quite suitable for enhancing photocatalytic degradation of pollutants. The experiments conducted for the determination of stability of coated N-doped TiO₂ polyscales in aqueous medium was found to be neglected, and it confirmed the strong adherence of N-doped TiO₂ on the surface of the supporting substrates. As Fig. 5 presents, the N-doped TiO₂ particles are heterogeneous morphology, i.e., a mixture of nano- and microscale; hence, the term polyscale was used to define the size nature of the N-doped TiO₂ particles.

**Fig. 5** SEM image of coated N-doped TiO₂ polyscales onto **a** ceramic beads supporting substrate; **b** thermocol beads supporting substrates

The photocatalytic activity of coated N-doped TiO₂ polyscales was determined using a model dye, brilliant green (Himedia, laboratory grade), under visible light

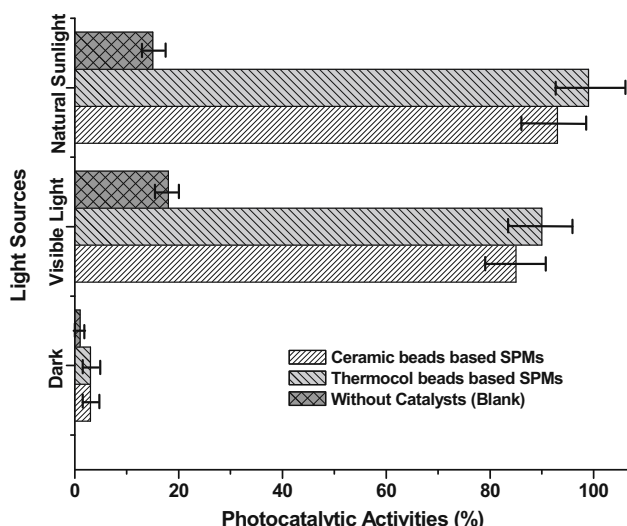


Fig. 6 Photocatalytic activities of coated N-doped TiO₂ polyscales under the different light sources

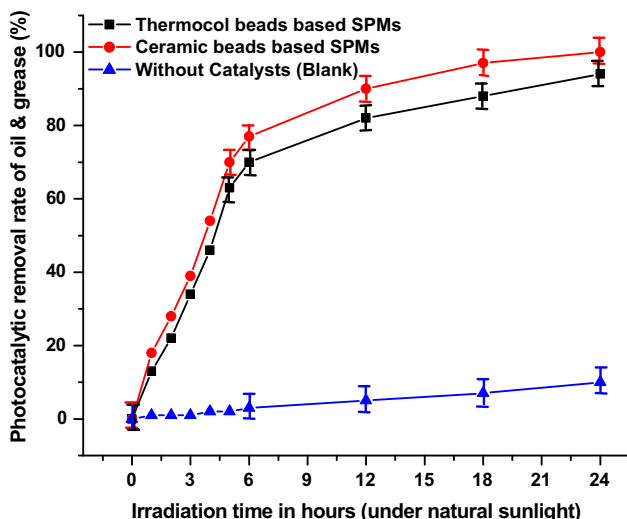


Fig. 7 Photocatalytic removal rate of oil and grease contamination in the aqueous media

source (100 W Tungsten bulb) and natural sunlight illumination. Natural sunlight illumination was showed an average exposure value of 9.72×10^3 lx which is comparatively greater than artificial visible light source (3.62×10^3 lx) which attributed higher removal efficiency under sunlight ($99 \% \pm 2$) than visible light sources ($93 \% \pm 2$) which can be seen in Fig. 6. Simultaneously, blank experiments were also maintained without coated N-doped TiO₂ polyscales. Both ceramic and thermocol beads based on coated N-doped TiO₂ polyscales exhibited efficient photocatalytic activities under both light sources. Ceramic bead-based coated N-doped TiO₂ polyscales showed comparatively higher photocatalytic activities (8–10 %) than the thermocol-based coated N-doped TiO₂ polyscales under different light sources. This could be attributed to the high porosity and surface areas of ceramic beads, which induce the interaction and contact rate between the organic molecules and photocatalyst in the ceramic bead-based, coated N-doped TiO₂ polyscales (Fig. 6).

Photocatalytic degradation of oil and grease

The photocatalytic degradation of oil and grease contamination alone in the aqueous media (model sample) was carried out using coated N-doped TiO₂ polyscales under natural sunlight illumination as an alternative driving energy source. The experiments were carried out for 6-h duration and continued up to 24 h by irradiating the samples to natural sunlight for 6 h on each day ($\approx 9.72 \times 10^3$ lx). Both the ceramic and thermocol beads-based coated N-doped TiO₂ polyscales showed the potential degradation efficiencies up to $100 \% \pm 2$ and $94 \% \pm 2$, respectively, for 24-h irradiation time. The ceramic bead-based coated N-doped TiO₂ polyscales showed comparatively higher degradation efficiency ($>10 \%$) than the thermocol-based coated N-doped TiO₂

Table 1 Photocatalytic removal rate of chemical oxygen demand using supported photocatalytic materials under natural sunlight

Irradiation time (h)	Removal of COD level (mg/l) under natural sunlight using supported photocatalyst		
	Blank (without catalyst)	N-doped TiO ₂ polyscales coated thermocol beads	N-doped TiO ₂ polyscales coated ceramic beads
0	10,400	10,400	10,400
1	10,296	9256	8528
2	10,192	8320	7280
3	10,088	7072	5928
4	9984	6136	4784
5	9880	5616	3744
6	9880	3952	3120
12	9776	2496	1664
18	9464	1768	832
24	9152	1396	490

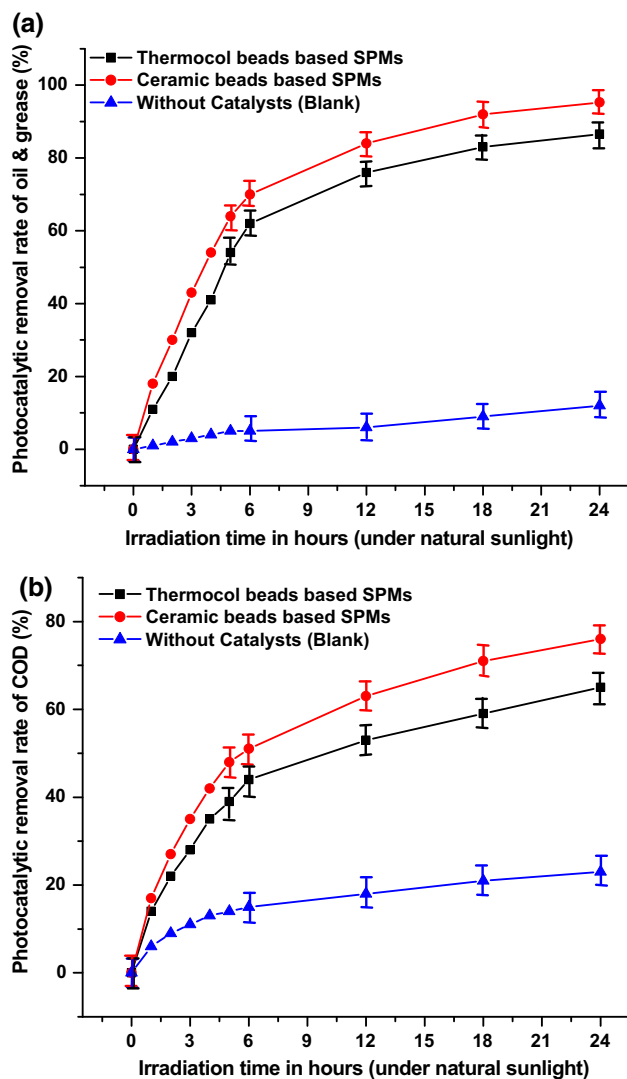


Fig. 8 Photocatalytic degradation efficiency of coated N-doped TiO₂ polyscales in the removal of **a** oil and grease in real-time wastewater; **b** COD in real-time wastewater

polyscales, and the degradation efficiency of oil and grease in aqueous media is shown in Fig. 7.

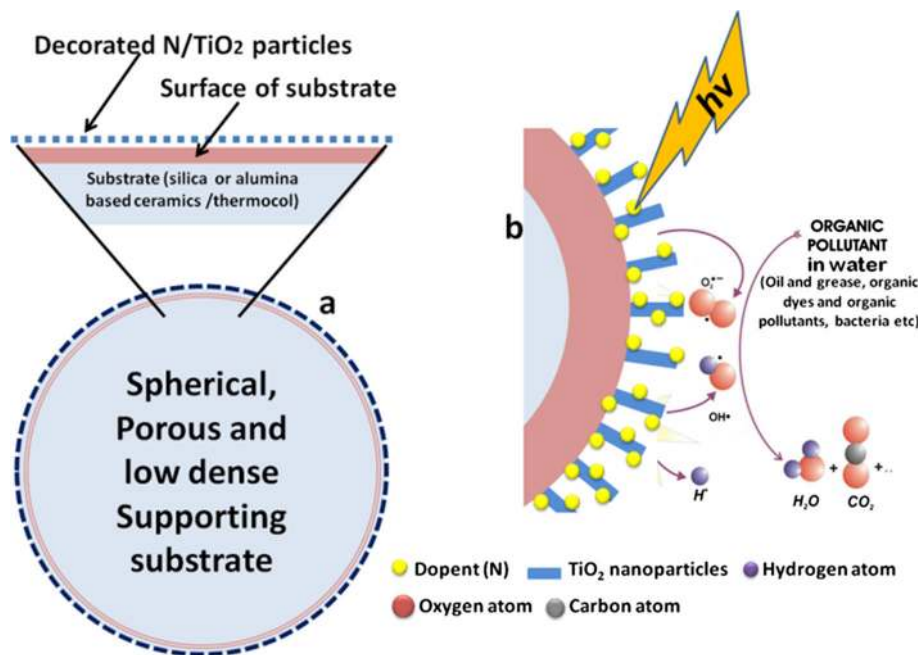
The photocatalytic treatment of oil and grease in the real-time industrial wastewater was carried out using ceramic and thermocol beads-based coated N-doped TiO₂ polyscales under natural sunlight illumination, and the degradation efficiency was 86.57 % ± 2 and 95.28 % ± 2, respectively, for 24-h irradiation time. In addition to the removal of oil and grease contamination in the wastewater, both coated N-doped TiO₂ polyscales showed potentiality reduction of COD level in the wastewater after photocatalytic treatment under natural sunlight illumination. The photocatalytic treatment efficiency of coated N-doped TiO₂ polyscales in removal of

oil and grease and in reduction of COD level (Table 1) in the real-time wastewater is shown in Fig. 8a, b, respectively. Moreover, the research revealed that both coated N-doped TiO₂ polyscales showed comparatively higher degradation efficiency (5–6 %) in the model aqueous medium than the real-time wastewater. Perhaps this happened due the other contaminants that reduce the photocatalytic activities by reduction in the irradiation rate by obstructing the light waves to reach the surface of photocatalyst. The reduction in COD level in the wastewater confirmed the photocatalytic degradation of oil and grease contamination along with the other organic pollutants in the wastewater. Apparently, coated N-doped TiO₂ polyscales can be utilized as potential catalysts by harvesting the natural sunlight as a renewable and potential alternative driving energy for the treatment of water and wastewater.

The coated N-doped TiO₂ polyscales used in the present study have special features like a less denser and spherical shape that helps to float on the surface of water and apparently enhance the degradation rate of oil and grease which floats on the surface (Shivaraju et al. 2010a, b; Muhammad et al. 2013; Nangrejo et al. 2008; Zhongxin et al. 2014; Han-Yu et al. 2015; Yeon et al. 2001; Hawley et al. 1984; Jinzhou et al. 2015). Due to lesser dense and spherical in shape, irradiation rate of the coated N-doped TiO₂ polyscales to the light will be enhanced gradually and also achieve high contact rate between pollutants and catalytic active sites by easy rotation through the terrestrial winds in the ambient environment (Shivaraju et al. 2010a, b; Muhammad et al. 2013; Nangrejo et al. 2008; Zhongxin et al. 2014; Han-Yu et al. 2015; Yeon et al. 2001; Faisal et al. 2007). Therefore, the composition of supporting substrates and multifunctional design of coated N-doped TiO₂ polyscales provide higher contacting rate and addition kinetic energy that enhances the overall degradation rate of oil and grease molecules along with the other organic pollutants in water and wastewater (Shivaraju et al. 2010a, b; Muhammad et al. 2013; Nangrejo et al. 2008; Boudjemaa et al. 2016; Shivaraju 2011). The schematic of multifunctional coated N-doped TiO₂ polyscales and photocatalytic degradation mechanism is illustrated in Fig. 9. The present study revealed that both coated N-doped TiO₂ polyscales presented considerable degradation efficiency by utilizing natural sunlight, which is cost-effective, pollution free, and also reduces the dependency on the convention energy sources for the water and wastewater treatment purposes. In addition, coated N-doped TiO₂ polyscales were found to be easily recovered after the completion of treatment and were easy to handle without any sophisticated infrastructure.



Fig. 9 Schematic of multifunctional coated N-doped TiO₂ polyscales design and its photocatalytic degradation mechanism



Conclusion

The present study addressed the preparation of the potential visible light responsive coated N-doped TiO₂ polyscales through sol–gel technique. The characterization results revealed well-crystalline phase, desired structural elucidation and morphology, considerable shifting and narrowing of bandgap energy from 3.22 to 3.12 eV, and higher photocatalytic activities (92–99 % ± 2) in coated N-doped TiO₂ polyscales. Multifunctional coated N-doped TiO₂ polyscales were successfully designed using thermocol and ceramic beads as the potential supporting substrates that enhanced the overall photocatalytic degradation efficiency under natural sunlight illumination along with the easy recovery and handling. Moreover, coated N-doped TiO₂ polyscales confirmed the up to 96 % ± 2 and 100 % ± 2 removal efficiency of oil and grease in both model and real-time wastewater, respectively, under the renewable and alternative energy sources like natural sunlight. N-doped TiO₂ polyscale-assisted treatment techniques with desired fabrication will be substituting the conventional and inefficient treatment methods in the removal of oil and grease and other organic contaminants in the polluted water bodies under the natural sunlight.

Acknowledgments The authors would like to thank for the support of Mr. Anil Kumar KM and Mr. Midhun G, Pallavi S, and Pallavi N, Research scholars in wet laboratory experiments and characterization, and it is highly appreciated. Inputs of Prof. S Suriyanarayanan, the Head of Department, greatly helped improve the manuscript that for which we are grateful.

References

- Adeola AA, McMartin DW, Angus B (2012) Environmental contamination of ready meals by polychlorinated biphenyls (PCBs). *J Environ Sci Heal A* 47(14):2230–2240
- Agota H, Behzad M, Patricia AS (2012) Seasonal monitoring of hydrocarbon degraders in Alabama marine ecosystems following the deepwater horizon oil spill. *Water Air Soil Pollut* 223(6):3145–3154
- Andreozzi R, Caprio V, Inola AM (1999) Advanced oxidation processes (AOP) for water purification and recovery. *Catal Today* 53:51–59
- APHA, AWWA, WEF (2015) Standards method for the examination of water and wastewater, 22nd edn. American Public Health Association, Washington
- Asahi R, Morikawa T, Ohwaki T, Aoki K, Taga Y (2001) Visible-light photocatalysis in nitrogen-doped titanium dioxide. *Science* 293:269–271
- Boudjemaa G, Abdelhamid H, Ferhat B, Noureddine B (2016) Elaboration and characterization of ceramic membrane supports from raw materials used in microfiltration. *Desali Water Treat* 57(12):5241–5245
- Brubaker D (1993) Marine pollution and international law: principles and practice. Belhaven Press, London, pp 234–245
- Cooney JJ (1984) The fate of petroleum pollutants in freshwater ecosystems. An atlas of petroleum microbiology. Macmillan publishing company, New York, pp 355–398
- Emerson CK, Maximiliano JMZ, Renato VG, Sherdil K, de Mauricio OV, Jairton D, Sérgio R, Marcos JLS (2015) Polymorphic phase study on nitrogen-doped TiO₂ nanoparticles: effect on oxygen site occupancy, dye sensitized solar cells efficiency and hydrogen production. *RSC Adv* 123:101276–101286
- Ergo R, Zekker I, Martin T, Priit V, Kristel K, Alar S, Taavo T, Anne M, Liis L, Sergio SC, Rubin DC, Toomas T (2014) Comparison of sulfate-reducing and conventional Anammox upflow anaerobic sludge blanket reactors. *J Biosci Bioengine* 118(4):426–433



- Faisal IH, Kazuo Y, Kensuke F (2007) Hybrid treatment systems for dye wastewater, critical reviews. *Environ Sci Technol* 37(4):315–377
- Gennaro M (2004) Oil pollution liability and control under international maritime law: market incentives as an alternative to government regulation. *Vand J Transnat'l L* 37(1):265–298
- Gomathi Devi L, Kavitha R (2014) Review on modified N–TiO₂ for green energy applications under UV/visible light: selected results and reaction mechanisms. *RSC Adv* 4:28265–28299
- Han-Yu H, Cheng-Thai Y, Rong-Ming H (2015) Well-ordered nanohybrids and nanoporous materials from gyroid block copolymer templates. *Chem Soc Rev* 44:1974–2018
- Hassan A (1989) Oil contamination in the Red sea environment. *Water Air Soil Pollut* 45(3):235–242
- Hawley F, Parson ML, Karasek FW (1984) Products obtained during combustion of polymers under simulated incinerator conditions II. Polystyrene. *J Chromotogr* 315:201–210
- Ihara T, Miyoshi M, Triyama Y, Marsumato O, Sugihara S (2003) Visible-light-active titanium oxide photocatalyst realized by an oxygen-deficient structure and by nitrogen doping. *Appl Catal B* 42:403–409
- Irie H, Watanabe Y, Hashimoto K (2003) Nitrogen-concentration dependence on photocatalytic activity of TiO₂-xNx powders. *J Phys Chem B* 107(23):5483–5486
- Jin Zhou Z, Zuolei L, Yongming L (2015) Preparation and characterization of low-density mullite-based ceramic proppant by a dynamic sintering method. *Mat Lett* 152:72–75
- Kulik N, Trapido M, Veressinina Y, Munter R (2007) Treatment of surfactant stabilized oil-in-water emulsions by means of chemical oxidation and coagulation. *Environ Technol* 28(12):1345–1355
- Laszlo ZK, Lajos K, Keszthelyi-Szabo G, Hodur C, Laszlo Z (2015) Treatment of oily wastewater by combining ozonation and microfiltration. *Desalin Water Treat* 55(13):3662–3669
- Lepo LE, Cripe CR, Kavanaugh JL, Zhang S, Norton GP (2003) The effect of amount of crude oil on extent of its biodegradation in open water- and sandy beach-laboratory simulations. *Environ Technol* 24(10):1291–1302
- Mehmet LY, Tanju E, Necip A (2014a) A novel efficient photocatalyst based on TiO₂ nanoparticles involved boron enrichment waste for photocatalytic degradation of atrazine. *Chem Eng J* 250:288–294
- Mehmet LY, Tanju E, Necip A, Shaobin W (2014b) Adsorptive and photocatalytic removal of reactive dyes by silver nanoparticle-colemanite ore waste. *Chem Eng J* 242:333–340
- Muhammad AZ, Deana W, Sinta L (2013) Adsorption of lignosulfonate compound from aqueous solution onto chitosan-silica beads. *Sep Sci Technol* 48(9):1391–1401
- Nangrejo M, Ahmad Z, Stride E, Edirisinghe M, Colombo P (2008) Preparation of polymeric and ceramic porous capsules by a novel electrohydrodynamic process. *Pharm Dev Technol* 13(5):425–432
- National academy of sciences (1985) Oil in the sea: inputs, fates and effects. National Academy Press, Washington
- O'Brien PY, Peter SD (1976) The effects of oils and oil components on algae: a review. *Brit Phycol J* 11(2):115–142
- Olumide AS, Morgan A, Peter KJR, Ling SW, McCullagh C (2011) Remediation of oily wastewater from an interceptor tank using a novel photocatalytic drum reactor. *Desalin Water Treat* 26:1–3
- Pera-Titus M, Garcia-Molina V, Banos MA, Gimenez S, Esplugas S (2004) Degradation of chlorophenols by means of advanced oxidation processes: a general review. *Appl Catal B Environ* 47:219–256
- Rodrigo A, Tara LC, Edward JB (2016) How much crude oil can zooplankton ingest? Estimating the quantity of dispersed crude oil defecated by planktonic copepods. *Environ Pollut* 208(B):645–654
- Rosario I, Rosa MF, Luis GT (2003) Soil and water contamination levels in an out-of-service oil distribution and storage station in Michoacan, Mexico. *Water Air Soil Pollut* 146(1):261–281
- Sadler R, Olszowy H, Shaw G, Biltoft R, Connell D (1994) Soil and water contamination by arsenic from a tannery waste. *Water Air Soil Pollut* 78(1):189–198
- Savita D, Suchi T (2007) Effects of religious practices on water quality of Shahpura Lake, Madhya Pradesh, India. *Water Int* 32(1):889–893
- Shivaraju HP (2011) Preparation and characterization of supported photocatalytic composite and its decomposition and disinfection effect on bacteria in municipal sewage water. *Res J Chem Sci* 1(2):56–63
- Shivaraju HP, Byrappa K, Vijay Kumar TMS, Ranganathaiah C (2010a) Hydrothermal synthesis and characterization of TiO₂ nanostructures on the ceramic support and their photo-catalysis performance. *Bull Catal Soc India* 9:37–50
- Shivaraju HP, Sajan CP, Rungnapa T, Kumar V, Ranganathaiah C, Byrappa K (2010b) Photocatalytic treatment of organic pollutants in textile effluent using hydrothermally prepared photocatalytic composite. *Mater Res Innov* 14(1):80–86
- Stolzenbach KD, Madsen OS, Adams EE, Pollack AM, Cooper CK (1977) A review and evaluation of basic techniques for predicting the behavior of surface oil slicks. Parsons Laboratory for Water Resources and Hydrodynamics, Cambridge, p 322
- Suresh Kumar M, Vaidya AN, Pandey RA, Shivaraman N, Bal AS (1996) Biological treatment of oil bearing wastewaters from steel industries—a case study. *J Environ Sci Heal Part A Environ Sci Eng Toxic* 31(1):167–181
- Syed S (2015) Approach of cost-effective adsorbents for oil removal from oily water, critical reviews. *Environ Sci Technol* 45(17):1916–1945
- Vinod KG, Tanju E, Necip A, Mehmet LY, Cemal P, Hassan KM (2015) CoFe₂O₄@TiO₂ decorated reduced graphene oxide nanocomposite for photocatalytic degradation of chlorpyrifos. *J Mol Liq* 208:122–129
- Willard EB, McDonald LL, Wallace PE, Mark V (1995) Effect of the Exxon Valdez oil spill on intertidal fish: a field study. *Trans Am Fish Soc* 124(4):461–476
- Yeon H, Hyo SL, Woo CL (2001) Preparation of low density ceramic support from coal fly ash. *Geosys Eng* 4(4):101–106
- Zekker I, Rikmann E, Tenno T, Priit V, Martin T, Menert A, Loorits L, Tenno T (2012) Anammox bacteria enrichment and phylogenetic analysis in moving bed biofilm reactors. *Environ Engine Sci* 29(10):946–950
- Zekker I, Ergo R, Toomas T, Kristel K, Priit V, Erik S, Liis L, Sergio CDCR, Siegfried V, Taavo T (2013) Deammonification process start-up after enrichment of anammox microorganisms from reject water in a moving-bed biofilm reactor. *Environ Technol* 34(23):3095–3101
- Zekker I, Rikmann E, Tenno T, Seiman A, Loorits L, Kroon K, Tomingas M, Vabamae P, Tenno T (2014) Nitrating-anammox biomass tolerant to high dissolved oxygen concentration and C/N ratio in treatment of yeast factory waste water. *Envi Technol* 35(9–12):1565–1576
- Zekker I, Ergo R, Toomas T, Liis L, Kristel K, Hannu F, Tero T, Priit V, Markus R, Anni M, Sergio CDCR, Taavo T (2015a) Nitric oxide for anammox recovery in a nitrite-inhibited deammonification system. *Environ Technol* 36(19):2477–2487
- Zekker I, Rikmann E, Tenno T, Kroon K, Seiman A, Loorits L, Fritze H, Tuomivirta T, Priit V, Raudkivi M, Mandel A, Tenno T (2015b) Start-up of low-temperature anammox in UASB from



- mesophilic yeast factory anaerobic tank inoculums. *Environ Technol* 36(2):214–225
- Zekker I, Rikmann E, Mandel A, Mandel A, Kroon K, Seiman A, Mihkelson J, Tenno T, Tenno T (2016) Step-wise temperature decreasing cultivates a biofilm with high nitrogen removal rates at 9 °C in short-term anammox biofilm tests. *Environ Technol* 37(15):1933–1946
- Zhongxin X, Yingze C, Na L, Lin F, Lei J (2014) Special wettable materials for oil/water separation. *J Mater Chem A* 2:2445–2460

